





Directed percolation in temporal networks

Arash Badie-Modiri ¹, Abbas K. Rizi ¹, Márton Karsai ^{2,3} and Mikko Kivelä ¹
¹*Department of Computer Science, School of Science, Aalto University, FI-0007 Espoo, Finland*
²*Department of Network and Data Science Central European University, 1100 Vienna, Austria*
³*Alfréd Rényi Institute of Mathematics, 1053 Budapest, Hungary*



(Received 18 October 2021; accepted 6 April 2022; published 25 May 2022)

Connectivity and reachability on temporal networks, which can describe the spreading of a disease, the dissemination of information, or the accessibility of a public transport system over time, have been among the main contemporary areas of study in complex systems for the last decade. However, while isotropic percolation theory successfully describes connectivity in static networks, a similar description has not yet been developed for temporal networks. Here, we address this problem and formalize a mapping of the concept of temporal network reachability to percolation theory. We show that the limited-waiting-time reachability, a generic notion of constrained connectivity in temporal networks, displays a directed percolation phase transition in connectivity. Consequently, the critical percolation properties of spreading processes on temporal networks can be estimated by a set of known exponents characterizing the directed percolation universality class. This result is robust across a diverse set of temporal network models with different temporal and topological heterogeneities, while by using our methodology we uncover similar reachability phase transitions in real temporal networks too. These findings open up an avenue to apply theory, concepts, and methodology from the well-developed directed percolation literature to temporal networks.

DOI: [10.1103/PhysRevResearch.4.L022047](https://doi.org/10.1103/PhysRevResearch.4.L022047)

Many dynamical processes evolving on networks are related to the problem of reachability. Reachability describes the existence of a possible path of connections between two nodes, denoting the possibility and the extent that one node can affect, cause a change in, or communicate with the others based on interactions represented in the network. The conception and formalism of reachability, however, change dramatically if one considers the time-varying nature of connections between nodes [1] as opposed to the classic static network modeling of systems where connections are considered constant. Time induces an inherent direction of connectivity, as it restricts the direction of influence or information flow. This in turn has an impact on many dynamical processes evolving on such networks, such as spreading [2–4], social contagion [5,6], *ad hoc* message passing by mobile agents [7], or routing dynamics [8]. In these processes, interacting entities may have limited memory, thereby only building up paths constrained by limited waiting times, further restricting the eligible temporal structure for their global emergence.

Directed percolation (DP) is a paradigmatic example to characterize connectivity in temporal systems. This process exhibits dynamical phase transitions into absorbing states with a well-defined set of universal critical exponents [9–12]. Since

its introduction [13] and during its further development [14], directed percolation has attracted considerable attention in the literature. It has applications in reaction-diffusion systems [15], star formation in galaxies [16], conduction in strong electric fields in semiconductors [17], and biological evolution [18]. While it is straightforward to define idealized models governed by directed percolation, such as lattice models [19–25], its features are more difficult to realize in nature [12,26], allowing only a few recent experimental realizations of directed percolation [27–29]. Nevertheless, this description is advantageous in providing an understanding of the connectivity of temporal structures to describe ongoing dynamical processes [30–40].

There is a thorough theoretical understanding of static network connectivity with several concepts borrowed from percolation theory, such as phase transitions, giant components, and susceptibility. These concepts, originally developed for lattices and random networks, are routinely used to analyze real-world networks and processes, e.g., disease spreading [41–45]. Connectivity is also a central property of temporal networks, with several recent techniques to characterize it, e.g., using limited-waiting-time reachability [46–50].

A mapping between the temporal reachability phase transition and directed percolation has been anticipated before. This is a straightforward intuition as directed percolation accounts for the time-induced inherent directionality that characterizes temporal networks. For the special cases of contact susceptible \rightarrow infected \rightarrow susceptible (SIS) and susceptible \rightarrow infected \rightarrow recovered \rightarrow susceptible (SIRS) processes, this mapping has been shown over a regular lattice structure with the assumption that the contact between nodes follows a

Published by the American Physical Society under the terms of the [Creative Commons Attribution 4.0 International](https://creativecommons.org/licenses/by/4.0/) license. Further distribution of this work must maintain attribution to the author(s) and the published article's title, journal citation, and DOI.

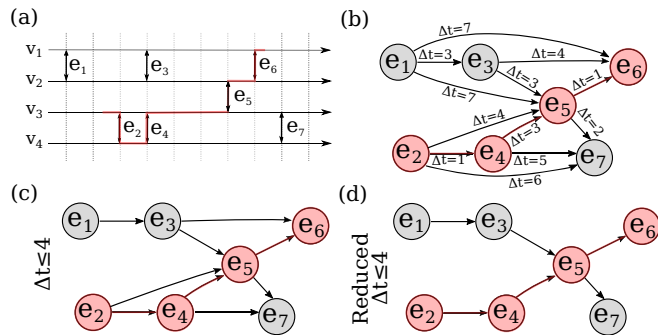


FIG. 1. Different representations of an instantaneous, undirected temporal network. (a) Vertices v_i are connected via dyadic instantaneous events e_j . (b) In a weighted temporal event graph, adjacent events are connected via links directed by time and weighted with the time difference Δt between them. Paths in an event graph are equivalent to time-respecting paths [56]. (c) Waiting-time constrained event graphs with links of weights $\Delta t \leq \delta t$ removed contain all δt -limited paths. (d) Reduced event graph in which locally redundant links are removed (see main text). The highlighted line represents a time respecting path (a) and its equivalent path over event graphs (b) and (c) and reduced event graph (d).

Poisson point process [9,12,51]. This mapping has been shown for a particular class of temporal dynamical systems, involving deterministic walks and discrete temporal layers [40]. For a more general class of temporal networks, Ref. [52] conjectured the mapping with directed percolation based on semantic similarities between the two systems and some empirical evidence. However, these studies could not provide conclusive evidence for this mapping for a broader set of temporal networks. In this Research Letter, we aim to show analytically that limited-waiting-time reachability on temporal networks, under a mean-field assumption of connectivity, has a phase transition in the directed percolation universality class. Combined with the experimental results of Ref. [53], we conclude that the same is true for a diverse subset of temporal networks, with a wider range of temporal and spatial connectivity compared with the mean-field assumption. Lastly, we illustrate how the directed percolation methodology, the formalism, and the introduced characteristic quantities can be used to analyze real-world temporal networks, for example, in detecting the onset of reachability phase transitions.

Modeling approach. A temporal network $G = (\mathcal{V}, \mathcal{E}, \mathcal{T})$ is defined as a set of nodes \mathcal{V} connected through events $e = (u, v, t_{\text{start}}, t_{\text{end}}) \in \mathcal{E}$, each of which represents an interaction of two nodes $u, v \in \mathcal{V}$ starting at time t_{start} and ending at time t_{end} observed during an observation period \mathcal{T} (i.e., $t_{\text{start}}, t_{\text{end}} \in \mathcal{T} \forall e \in \mathcal{E}$ and $t_{\text{start}} < t_{\text{end}}$). The connectivity of events is characterized by time-respecting paths [34,54], defined as sequences of adjacent events. Here, we call two distinct events $e, e' \in \mathcal{E}$ adjacent and denote this by $e \rightarrow e'$, if they follow each other in time ($t'_{\text{start}} > t_{\text{end}}$) and share at least one node in common ($\{v, u\} \cap \{v', u'\} \neq \emptyset$) as demonstrated in Fig. 1(a). For simplicity, we assume that temporal network events are instantaneous ($t_{\text{start}} = t_{\text{end}}$), but all of our notations can be easily extended to directed events and to temporal hypergraphs [47,55].

While time-respecting paths encode the possible routes of information, some dynamical processes have further restrictions on the duration they can propagate further after reaching a node. For example, in disease spreading, infected nodes may recover after some time, becoming unable to infect other nodes unless reinfected. In our definition, we define limited waiting times in temporal paths by allowing adjacent events $e = (u, v, t_{\text{start}}, t_{\text{end}})$ and $e' = (u', v', t'_{\text{start}}, t'_{\text{end}})$ to be connected (δt adjacent) only if there is less than δt time between them (i.e., $t'_{\text{start}} - t_{\text{end}} < \delta t$). In contrast to the control parameters based on node or event occupation probabilities, which could be used to adjust the overall activity level of the network, changing δt modifies the behavior of the spreading itself. Additionally, processes unconstrained by waiting time can be modeled as a special case of the limited-waiting-time process, with an infinitely large value of δt .

A compact way of describing the problem of reachability on temporal networks is provided by the weighted event graph representation $D = (\mathcal{E}, E_D, \Delta t(e, e'))$, a static directed acyclic representation of temporal networks [52]. In this description, events act as nodes, and two events e and e' are connected through a directed, weighted link if they are adjacent with weights defined as $\Delta t(e, e') = t'_{\text{start}} - t_{\text{end}}$, i.e., $E_D = \{(e, e') \in \mathcal{E} \times \mathcal{E} \mid e \rightarrow e'\}$. The event graph contains a superposition of all temporal paths [56] and retains the arrow of time even after turning the temporal structure into a static one [Fig. 1(b)]. Event graph representation of temporal networks has proven to be suitable for studying properties of temporal networks such as occurrences of motifs [57], decomposition of the temporal network into smaller components [58], and providing a lower-dimensional embedding of the temporal network that can be consumed by many machine-learning methods [59]. For our use case, a superposition of all δt -limited-time temporal paths ($D_{\delta t}$) of the temporal network can be achieved by constructing the event graph of the temporal network and removing all the event graph links with weights larger than δt ; in other words, $D_{\delta t}$ is a directed graph with the same set of vertices and the same weight function as D and set of edges $\{(e, e') \in E_D \mid \Delta t(e, e') \leq \delta t\}$ [see Fig. 1(c)].

Furthermore, we define the reduced temporal event graph \hat{D} and its waiting-time constrained variation $\hat{D}_{\delta t}$, where only the first adjacency relationships per temporal network node for each event are retained. \hat{D} and $\hat{D}_{\delta t}$ nodes have a maximum in- and out-degree of 2, yet they contain all the reachability relationships of the original event graph [60]. That is, the reduced event graph exactly retains the reachability of the original event graph by removing redundant connections (feed-forward loops) between events. The reduction allows interpretation of the three possible out-degrees using the terminology of directed percolation as annihilation (0), diffusion (1), and decoagulation (2) in the case that the out-neighbors are not already reachable through some longer loop. Note that this upper bound on in- and out-degrees is valid if the probability of simultaneous occurrence of adjacent events is negligible. See Supplemental Material (SM) for more details [61].

Order parameters and other characteristics. Compared with static structures, temporal networks incorporate time as an additional degree of freedom, which introduces an extra dimension to the characterization of their structural phase

transition of connectivity around a critical point. This is similar to directed percolation, where dimensions are related to space and time with associated independent critical exponents [62,63]. We measure the expected δt -limited-waiting-time reachability starting from a random event e . Of interest is the number of unique reachable nodes $\mathcal{V}_{e \rightarrow} \subseteq \mathcal{V}$, the time duration of the longest path (i.e., its lifetime [52]) $\mathcal{T}_{e \rightarrow} \subseteq \mathcal{T}$, and the total number of reachable events $\mathcal{M}_{e \rightarrow} \subseteq \mathcal{E}$. The expected values of these are analogous to the mean spatial volume $V = \langle |\mathcal{V}_{e \rightarrow}| \rangle$, mean survival time $T = \langle \max \mathcal{T}_{e \rightarrow} - \min \mathcal{T}_{e \rightarrow} \rangle$, and mean cluster mass $M = \langle |\mathcal{M}_{e \rightarrow}| \rangle$ in the directed percolation formalism (respectively) [9,12]. Furthermore, in parallel to directed percolation, we define the survival probability $P(t)$ as the probability that there is a path from a randomly selected initial source event at t_0 to an event after time $t_0 + t$. The ultimate survival probability $P_\infty = \lim_{t \rightarrow \infty} P(t)$ is then the survival probability at large values of t . Note that when defining these quantities, we opted for simplicity (see Supplemental Material [61] for discussion).

Using the maximum waiting time δt as a control parameter is a natural choice as it has a clear physical interpretation. However, unlike occupation probabilities that are typically used as control parameters in directed percolation, the scale of δt depends on the timescales of the system. Furthermore, although it is related to the local connectivity, this relationship is indirect and might depend on, e.g., the temporal inhomogeneities in interaction sequences. For this reason, we define another control parameter that directly measures the local connectivity of the system. We use the local effective connectivity $\hat{q}^{\text{out}}(\delta t)$, which is the average excess out-degree of the reduced event graph $\hat{D}_{\delta t}$. This is a monotonically increasing function of δt , which normalizes the changes in connectivity given by the changes in the maximum allowed waiting time δt . We then centralize this quantity by subtracting its value from its phase-transition critical point \hat{q}_c^{out} and denote the resulting control parameter as $\tau = \hat{q}^{\text{out}} - \hat{q}_c^{\text{out}}$.

In addition to the single-source scenario, where the component starts from a single node in $D_{\delta t}$, we investigated the fully occupied homogeneous initial condition, where we compute paths starting from all nodes in $D_{\delta t}$ with time $t < t_0$. Analogous to directed percolation, we define particle density $\rho(t)$ as the fraction of infected nodes in $D_{\delta t}$ at time t , while stationary density $\rho_{\text{stat}}(\tau)$, the order parameter, is defined as the particle density after the system reached a stationary state. We can incorporate the effects of an external field h into this scenario: In continuous time, this would be equivalent to the spontaneous emergence of sources of infection, i.e., occupation, of nodes in $D_{\delta t}$ (events in G) through an independent Poisson point process with rate h . Susceptibility $\chi(\tau, h) = \frac{\partial}{\partial h} \rho_{\text{stat}}(\tau, h)$ can then be measured through observing the effect of changing the external field [12].

Critical behavior in random systems. Next, we derive a mean-field approximation for the above-defined measures and identify the critical point. We model temporal networks with an underlying static structure, where events are induced via links activating by independent and identical continuous-time stochastic processes. In order to do so, we need to first derive the degree distribution of the reduced event graph $\hat{D}_{\delta t}$, i.e., probabilities that one can reach zero, one, or two events from a randomly chosen event in the temporal network. Given the

excess degrees l and r of the two temporal network nodes in G incident to the link corresponding to the event $e \in \mathcal{E}$, we can compute the probability of a zero out-degree for a node in $\hat{D}_{\delta t}$ (i.e., an event in original temporal network G) as $\hat{p}_0^{\text{out}} = \Pi_{\delta t} \hat{\Pi}_{\delta t}^{l+r}$. Here, $\Pi_{\delta t}$ is the cumulative interevent time distribution induced by a link activation process for a given δt , and $\hat{\Pi}_{\delta t}$ is the corresponding cumulative residual interevent time distribution. Similarly, for out-degree 2, we can compute $\hat{p}_2^{\text{out}} = \int_0^\infty (1 - \hat{\Pi}_{\min \delta t, t}^l)(1 - \hat{\Pi}_{\min \delta t, t}^r) \pi_t dt$, where π_t is the interevent time distribution. Given that the maximum out-degree of events in the reduced event graph is 2, the \hat{p}_1^{out} can be derived as $\hat{p}_1^{\text{out}} = 1 - \hat{p}_0^{\text{out}} - \hat{p}_2^{\text{out}}$. In-degree probabilities can be derived similarly.

The joint in- and out-degree distribution of the event graph can be computed from the excess degree distribution q_k of the underlying static network. If the degrees are independent, this becomes $\hat{p}_{i,o}^{\text{in,out}} = \sum_{l,r} \hat{p}_l^{\text{in}} \hat{p}_o^{\text{out}} q_l q_r$. We will denote the generating function of the joint degree distribution as $\mathcal{G}_0(z_{\text{in}}, z_{\text{out}})$ and the corresponding excess out-degree distribution as $\mathcal{G}_1^{\text{out}}(z_{\text{out}})$. We construct the mean-field rate equation for occupation density $\rho(t)$ in the homogeneous occupation initial condition using the excess out-degree distribution of the event graph $\hat{q}_k^{\text{out}} = \frac{d^k}{k! dz^k} \mathcal{G}_1^{\text{out}}(z)|_{z=0}$. The excess out-degree of nodes in the event graph \hat{D} gives the change in the number of further nodes we can reach from an already reached node: Nodes with out-degree 2 increase the number of reached nodes by 1, nodes with out-degree 1 do not affect the number of reached nodes, and nodes with out-degree 0 reduce by 1 the number of reached nodes. The total change therefore is $\hat{q}_2^{\text{out}} - \hat{q}_0^{\text{out}}$. In addition, some nodes we can reach are already reachable through other paths. In total we reach on expectation $\hat{q}_1^{\text{out}} + 2\hat{q}_2^{\text{out}}$ nodes where each node is already reached with probability $\rho(t)$. The rate equation becomes

$$\partial_t \rho(t) = [\hat{q}_2^{\text{out}} - \hat{q}_0^{\text{out}}] \rho(t) - [\hat{q}_1^{\text{out}} + 2\hat{q}_2^{\text{out}}] \rho^2(t). \quad (1)$$

In this equation the values of \hat{q}_k^{out} are constants in time. Noting the critical point for this equation as $\hat{q}_2^{\text{out}} - \hat{q}_0^{\text{out}} = 0$ and noting that the expected value is by definition $\hat{q}^{\text{out}} = \hat{q}_1^{\text{out}} + 2\hat{q}_2^{\text{out}}$ and that $\hat{q}_2^{\text{out}} - \hat{q}_0^{\text{out}} = \hat{q}^{\text{out}} - 1$, we can write Eq. (1) as $\partial_t \rho(t) = \tau \rho(t) - \hat{q}^{\text{out}} \rho^2(t)$.

Equation (1) follows the same form as the directed percolation mean-field equation for a $(d+1)$ -dimensional lattice [12] and can be solved explicitly (see Supplemental Material [61]). It has the critical point at $\tau = 0$, while it indicates that $\rho \rightarrow \tau / \hat{q}^{\text{out}}$ for $\tau > 0$. Asymptotically, it provides the critical exponents as $\rho(t) \sim t^{-\alpha}$ at $\tau = 0$ and $\rho_{\text{stat}}(\tau) \sim \tau^\beta$ when $\tau > 0$ and $t \rightarrow \infty$ with values $\alpha = \beta = 1$, where $\alpha = \beta / \nu_{\parallel}$ and ν_{\parallel} is the temporal correlation length exponent, in accordance with the corresponding mean-field directed percolation critical exponents [12].

The expected out-component size, i.e., mean cluster mass M , can be computed from the joint degree distribution of the event graph $\hat{D}_{\delta t}$ by assuming that it is a random directed graph with the same joint in- and out-degree distribution as $\hat{D}_{\delta t}$. The out-component size distribution probability-generating function H_0 can be derived from $H_0(z_{\text{out}}) = z_{\text{out}} \mathcal{G}_0(1, H_1(z_{\text{out}}))$, $H_1(z_{\text{out}}) = z_{\text{out}} \mathcal{G}_1^{\text{out}}(H_1(z_{\text{out}}))$, and the mean out-component size can be written as $M = \frac{\partial H_0(z_{\text{out}})}{\partial z_{\text{out}}}|_{z_{\text{out}}=1}$ [64]. These equations, when $\tau \rightarrow 0^-$, lead to $M \sim -\tau^{-\gamma}$ with $\gamma = 1$ (see

Supplemental Material [61]). Here, $\gamma = \nu_{\parallel} + d\nu_{\perp} - \beta - \beta'$, matching the mean-field exponent of mean cluster mass in directed percolation [12]. Here, ν_{\perp} indicates the spatial temporal correlation exponent.

The component survival probability $P(t)$ is measured by the out-component time span of nodes in the event graph, and the occupation density $\rho(t)$ is calculated by the in-component sizes of all possibly reachable nodes, implying that these two quantities are equal, $\rho(t) = P(t)$ (see Supplemental Material [61]). Consequently, given the control parameter τ , $\rho_{\text{stat}}(\tau) = P_{\infty}(\tau)$ as long as the time-reversed event graph has the same probability of being generated as the original one (e.g., if $\forall_{i,o} p_{i,o}^{\text{in,out}} = p_{o,i}^{\text{in,out}}$). This leads us to the rapidity-reversal symmetry for event graphs similarly characterizing directed percolation [65] where $\beta = \beta'$ and $P_{\infty}(\tau) \sim \tau^{\beta'}$. Note that while the condition above holds for a variety of random temporal network models, for real-world systems intuition might suggest, e.g., a higher probability of $p_{1,2}^{\text{in,out}}$ as compared with $p_{2,1}^{\text{in,out}}$ due to over-representation of causal motifs [57]. In practice, however, we observed no deviations from the above condition in two large real-world systems (see Supplemental Material [61]).

Finite-size scaling in random systems. The critical exponents can be empirically verified through finite-size scaling of the system close to its percolation critical point, where its large-scale properties become invariant under scale transformations. We simulate random temporal networks of varying size and perform efficient reachability estimations [47] from single-source and homogeneous fully occupied initial conditions. We expect that curves of macroscopic quantities collapse when using the correct critical exponents of β , ν_{\parallel} , and ν_{\perp} corresponding to the mean-field values of directed percolation. The results confirm that the directed percolation mean-field exponents characterize the percolation phase transition of random temporal networks. This is demonstrated in Figs. 2(a)–2(f) for temporal networks induced on a 9-regular network with links activated via independent Poisson processes. These results are robust in the presence of several types of temporal and spatial heterogeneities [53].

Directed percolation measures in real-world temporal networks. We measure the same macroscopic quantities as before for four different real-world systems, concentrating on temporal networks describing air transportation, public transportation, Twitter mentions, and mobile phone calls [Figs. 3(a)–3(d)], respectively]. In these networks, an event represents a flight between two airports in the United States, a public transport vehicle transiting between two consecutive stations on a typical Monday in Helsinki, a user mentioning another user in a tweet on Twitter, and a mobile phone subscriber calling another subscriber of a major European carrier, respectively. For details of the data sets, see Table S1 of the SM. In each system, there is clear evidence of an absorbing to active phase transition in terms of M , V , and ρ_{stat} . Note that the scales of these quantities are not directly comparable, highlighting the fact that distinguishing between the different notions of connectivity is important in practical terms. Furthermore, multiple peaks in susceptibility indicate multiple connectivity timescales.

The reachability phase transition can be better understood by investigating temporal connectivity profiles represented by

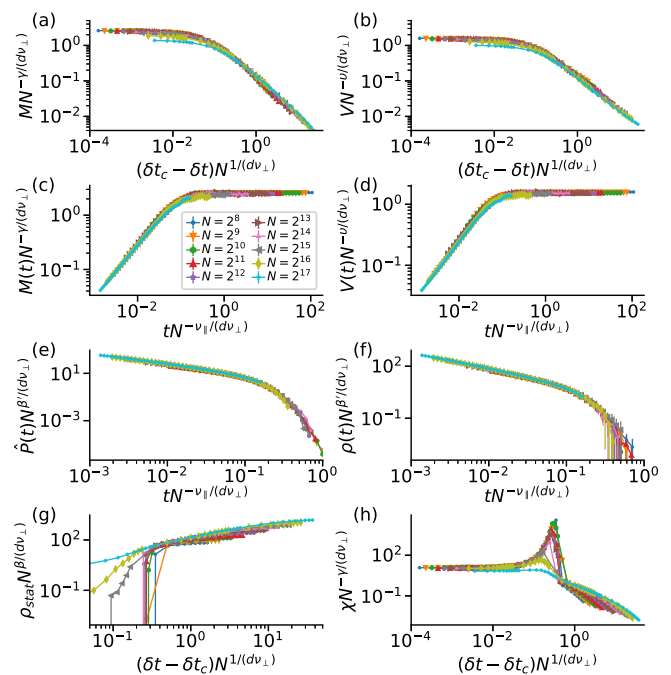


FIG. 2. Finite-size scaled (a) and (c) mean cluster mass M , (b) and (d) volume V , and (e) survival probability $\hat{P}(t)$ for single-source spreading scenarios. (f) Particle density $\rho(t)$, (g) static density ρ_{stat} , and (h) susceptibility $\chi(\delta t, 0)$ as a function of δt for the homogeneous initial condition. Measurements are averaged over at least 256 (up to 4096) realizations of temporal network constructed from random 9-regular networks ($N \in \{2^8, \dots, 2^{17}\}$) and Poisson point process activations $\lambda = 1$ of links. All functions of time are measured at $\delta t = \delta t_c = 0.08808$. d is set to directed percolation upper critical dimension $d_c = 4$.

cluster volumes of individual events. Structures similar to those of random networks (see Supplemental Material [61]) can be observed for air transport and Twitter [Figs. 3(e) and 3(g)]. However, in air transport, the structure is regular, following the diurnal pattern of flights. In Twitter, the components do not reach most nodes due to the greater separation of temporal components, and their structure reflects the rare emergence of possible macroscopic cascades. Public transport (1 day) and mobile networks display a single winglike structure [Figs. 3(f) and 3(h)]. This is induced by early components that can reach a significant fraction of nodes, which are then joined by other components reaching smaller subsets. This is also indicated by the horizontal structures under the wings.

Conclusion. The connectivity of a network is an important measure of its resilience and an underlying concept for any dynamical process running on it. It encodes the possible transportation routes or paths of information diffusion and determines how misinformation or diseases spread in real-world settings. The connectivity of static networks and related dynamical processes are routinely analyzed within the framework of (isotropic) percolation theory [30,31,41] with methods borrowed from critical phenomena [9,70]. Furthermore, many natural or synthetic networks, ranging from the brain [71,72] or artificial neural networks [73] to geological phenomena [74] and urban systems [75] tend to self-organize their medium or their parameters or be optimized by outside

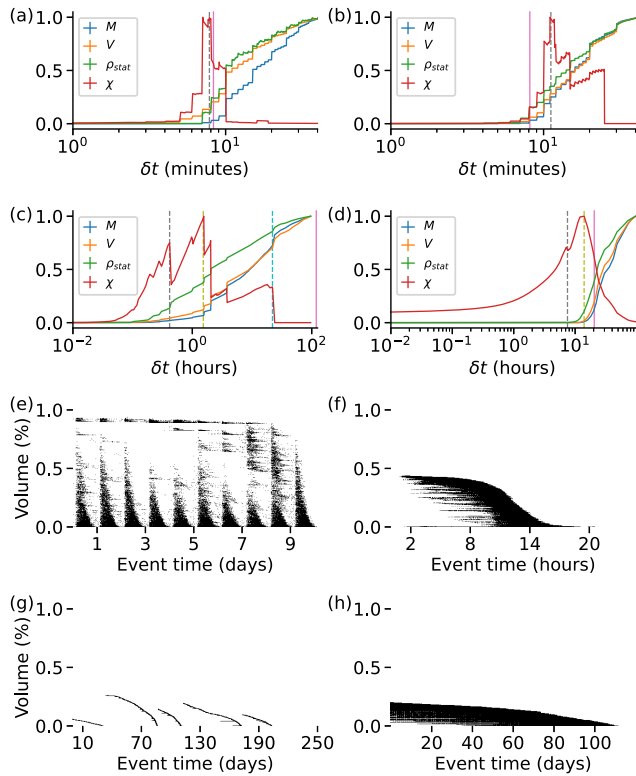


FIG. 3. Mean cluster mass M , mean cluster volume V , static density ρ_{stat} , and susceptibility $\chi(\delta t, 0)$ as a function of δt for four real-world networks: (a) Air transport [66], (b) Helsinki public transportation [67], (c) Twitter mentions [68], and (d) mobile phone calls [69] display an absorbing to active phase transition around 470 s, 670 s, 25 min, and 7.5 h, respectively, as indicated by change from very small values for M , V , and ρ_{stat} to values comparable to the size of the system and a peak in susceptibility $\chi(\delta t, 0)$. Mobile and Twitter networks show a second peak in susceptibility around 1.5 and 22 h, respectively, and Twitter data show a third peak around 14 h. The trajectories are rescaled to the range $[0, 1]$. δt_c is estimated using the analytical solution from Ref. [53] by approximating the network to a temporal network with a random regular static base and Poisson point process activation. This estimates the threshold at 500 s, 488 s, 119.1 h, and 22.5 h, respectively, displayed using solid vertical lines in (a)–(d). The temporal reachability profiles display relative cluster volumes for each event as a function of the event time for $\delta t \approx \delta t_c$ for (e) air transport, (f) Helsinki public transportation, (g) Twitter mentions, and (h) mobile phone call networks.

intervention towards criticality [76,77]. Therefore it is of great utility to locate the onset of critical phase-transition points and predict the behavior of the system in that vicinity.

While connectivity transitions and the critical behavior of the system are understood in static networks by means of isotropic percolation theory, temporal networks, by and

large, have been out of reach of a similar methodology. This has practical implications as connectivity is a limiting factor of any dynamical processes and at the same time temporal interactions have been shown to have dramatic effects on the speed and volume of any ongoing dynamical process [2–4]. For example, disease spreading in static networks can be mapped to a percolation process leading to a theoretical understanding of the epidemic threshold as a consequence of connectivity phase transition [41]. This connection has been extensively exploited to use the mathematical machinery of network percolation to derive various theoretical and practical results on static networks [31,78]. In temporal networks, such analysis is typically based on theoretical results on sequences of static networks [79] or case studies based purely on simulations [69,80]. The concise theory of temporal network connectivity provided here shows that the reachability phase transition in temporal networks belongs to the directed percolation universality class, which is a necessary step forward from the limited description provided by the theory of static networks. It also indicates that directed percolation may have many counterparts in reality with the expected scaling relations.

The mapping presented in this Research Letter allows for predicting the critical thresholds and the connectivity behaviors of a diverse set of systems that can be modeled as temporal networks. Now, similar to static network connectivity, not only do we have theoretically grounded summary statistics of the component size distribution (the order parameters and cluster mass, volume, and lifetime), but also we know ways to find their transitions even in finite-size systems. Moreover, we now possess a theory to predict the behavior of such random systems and find transition points accurately. Real networks are often approximated with random graphs, and the random models are used as reference points: Deviations from the minimal random models expose important structural features of the real systems, and conversely, agreement with these models tells us that the structures, correlations, and inhomogeneities present in the data do not have a measurable effect on the connectivity. Although introduction of heterogeneities might shift the critical threshold of connectivity in temporal networks, the directed percolation phase transition is surprisingly robust to several types of temporal and topological heterogeneities [53]. Consequently, further research is required to find the boundaries and extremities of application of this framework on theoretical and real-world networks.

Acknowledgments. We would like to thank János Kertész and Géza Ódor for their helpful comments and suggestions. The authors wish to acknowledge CSC – IT Center for Science, Finland, and the Aalto University “Science-IT” project for generous computational resources. M. Karsai acknowledges support from the DataRedux ANR project (ANR-19-CE46-0008) and the SoBigData++ H2020 project (H2020-871042).

[1] P. Holme and J. Saramäki, *Temporal Network Theory*, Computational Social Sciences (Springer, New York, 2019).
 [2] R. Lambiotte and N. Masuda, *A Guide to Temporal Networks* (World Scientific, Singapore, 2016), Vol. 4.

[3] P. Holme and J. Saramäki, Temporal networks, *Phys. Rep.* **519**, 97 (2012).
 [4] P. Holme, Modern temporal network theory: A colloquium, *Eur. Phys. J. B* **88**, 234 (2015).

- [5] D. J. Daley and D. G. Kendall, Epidemics and rumours, *Nature (London)* **204**, 1118 (1964).
- [6] C. Castellano, S. Fortunato, and V. Loreto, Statistical physics of social dynamics, *Rev. Mod. Phys.* **81**, 591 (2009).
- [7] C. Tripp-Barba, C. Alcaraz, and M. A. Igartua, Special issue on “Modeling and performance evaluation of wireless ad-hoc networks”, *Ad Hoc Networks* **52**, 1 (2016).
- [8] N. Nassir, M. Hickman, A. Malekzadeh, and E. Irannezhad, A utility-based travel impedance measure for public transit network accessibility, *Transp. Res. Part A: Policy Pract.* **88**, 26 (2016).
- [9] H. Hinrichsen, Non-equilibrium critical phenomena and phase transitions into absorbing states, *Adv. Phys.* **49**, 815 (2000).
- [10] G. Ódor, Universality classes in nonequilibrium lattice systems, *Rev. Mod. Phys.* **76**, 663 (2004).
- [11] H. Hinrichsen, Non-equilibrium phase transitions, *Physica A (Amsterdam)* **369**, 1 (2006).
- [12] M. Henkel, H. Hinrichsen, S. Lübeck, and M. Pleimling, *Non-equilibrium Phase Transitions* (Springer, New York, 2008), Vol. 1.
- [13] S. R. Broadbent and J. M. Hammersley, Percolation processes: I. Crystals and mazes, *Math. Proc. Cambridge Philos. Soc.* **53**, 629 (1957).
- [14] J. Blease, Directed-bond percolation on hypercubic lattices, *J. Phys. C: Solid State Phys.* **10**, 925 (1977).
- [15] F. Schlögl, Chemical reaction models for non-equilibrium phase transitions, *Z. Phys.* **253**, 147 (1972).
- [16] H. Gerola, P. Seiden, and L. Schulman, Theory of dwarf galaxies, *Astrophys. J.* **242**, 517 (1980).
- [17] N. Van Lien and B. Shklovskii, Hopping conduction in strong electric fields and directed percolation, *Solid State Commun.* **38**, 99 (1981).
- [18] P. Bak and K. Sneppen, Punctuated Equilibrium and Criticality in a Simple Model of Evolution, *Phys. Rev. Lett.* **71**, 4083 (1993).
- [19] E. Domany and W. Kinzel, Equivalence of Cellular Automata to Ising Models and Directed Percolation, *Phys. Rev. Lett.* **53**, 311 (1984).
- [20] W. Kinzel, Phase transitions of cellular automata, *Z. Phys. B: Condens. Matter* **58**, 229 (1985).
- [21] T. E. Harris, Contact interactions on a lattice, *Ann. Probab.* **2**, 969 (1974).
- [22] I. Jensen, Critical Behavior of the Pair Contact Process, *Phys. Rev. Lett.* **70**, 1465 (1993).
- [23] J. Mendes, R. Dickman, M. Henkel, and M. C. Marques, Generalized scaling for models with multiple absorbing states, *J. Phys. A: Math. Gen.* **27**, 3019 (1994).
- [24] R. M. Ziff, E. Gulari, and Y. Barshad, Kinetic Phase Transitions in an Irreversible Surface-Reaction Model, *Phys. Rev. Lett.* **56**, 2553 (1986).
- [25] D. Dhar, The collapse of directed animals, *J. Phys. A: Math. Gen.* **20**, L847 (1987).
- [26] H. Hinrichsen, On possible experimental realizations of directed percolation, *Braz. J. Phys.* **30**, 69 (2000).
- [27] K. A. Takeuchi, M. Kuroda, H. Chaté, and M. Sano, Directed Percolation Criticality in Turbulent Liquid Crystals, *Phys. Rev. Lett.* **99**, 234503 (2007).
- [28] G. Lemoult, L. Shi, K. Avila, S. V. Jalikop, M. Avila, and B. Hof, Directed percolation phase transition to sustained turbulence in Couette flow, *Nat. Phys.* **12**, 254 (2016).
- [29] M. Sano and K. Tamai, A universal transition to turbulence in channel flow, *Nat. Phys.* **12**, 249 (2016).
- [30] A. Barrat, M. Barthelemy, and A. Vespignani, *Dynamical Processes on Complex Networks* (Cambridge University Press, Cambridge, 2008).
- [31] R. Pastor-Satorras, C. Castellano, P. Van Mieghem, and A. Vespignani, Epidemic processes in complex networks, *Rev. Mod. Phys.* **87**, 925 (2015).
- [32] D. Kempe, J. Kleinberg, and A. Kumar, Connectivity and inference problems for temporal networks, *J. Comput. Syst. Sci.* **64**, 820 (2002).
- [33] J. Moody, The importance of relationship timing for diffusion, *Social Forces* **81**, 25 (2002).
- [34] P. Holme, Network reachability of real-world contact sequences, *Phys. Rev. E* **71**, 046119 (2005).
- [35] R. K. Pan and J. Saramäki, Path lengths, correlations, and centrality in temporal networks, *Phys. Rev. E* **84**, 016105 (2011).
- [36] I. Scholtes, N. Wider, R. Pfitzner, A. Garas, C. J. Tessone, and F. Schweitzer, Causality-driven slow-down and speed-up of diffusion in non-Markovian temporal networks, *Nat. Commun.* **5**, 5024 (2014).
- [37] J. Stehlé, N. Voirin, A. Barrat, C. Cattuto, L. Isella, J.-F. Pinton, M. Quaggiotto, W. Van den Broeck, C. Régis, B. Lina, and P. Vanhems, High-resolution measurements of face-to-face contact patterns in a primary school, *PLoS One* **6**, e23176 (2011).
- [38] S. Dai, H. Bouchet, A. Nardy, E. Fleury, J.-P. Chevrot, and M. Karsai, Temporal social network reconstruction using wireless proximity sensors: model selection and consequences, *EPJ Data Sci.* **9**, 19 (2020).
- [39] A. Aleta, G. F. de Arruda, and Y. Moreno, Data-driven contact structures: from homogeneous mixing to multilayer networks, *PLoS Comput. Biol.* **16**, e1008035 (2020).
- [40] R. Parshani, M. Dickison, R. Cohen, H. E. Stanley, and S. Havlin, Dynamic networks and directed percolation, *Europhys. Lett.* **90**, 38004 (2010).
- [41] M. E. J. Newman, Spread of epidemic disease on networks, *Phys. Rev. E* **66**, 016128 (2002).
- [42] E. Kenah and J. M. Robins, Second look at the spread of epidemics on networks, *Phys. Rev. E* **76**, 036113 (2007).
- [43] E. Kenah and J. C. Miller, Epidemic percolation networks, epidemic outcomes, and interventions, *Interdiscip. Perspect. Infect. Dis.* **2011**, 543520 (2011).
- [44] A. K. Rizi, A. Faqeh, A. Badie-Modiri, and M. Kivelä, Epidemic spreading and digital contact tracing: Effects of heterogeneous mixing and quarantine failures, *Phys. Rev. E* **105**, 044313 (2022).
- [45] T. Hiraoka, A. K. Rizi, M. Kivelä, and J. Saramäki, Herd immunity and epidemic size in networks with vaccination homophily, [arXiv:2112.07538](https://arxiv.org/abs/2112.07538).
- [46] P. Crescenzi, C. Magnien, and A. Marino, Approximating the temporal neighbourhood function of large temporal graphs, *Algorithms* **12**, 211 (2019).
- [47] A. Badie-Modiri, M. Karsai, and M. Kivelä, Efficient limited-time reachability estimation in temporal networks, *Phys. Rev. E* **101**, 052303 (2020).
- [48] A. Casteigts, A.-S. Himmel, H. Molter, and P. Zschoche, Finding Temporal Paths Under Waiting Time Constraints, *Algorithmica* **83**, 2754 (2021).
- [49] S. Thejaswi, J. Lauri, and A. Gionis, Restless reachability problems in temporal graphs, [arXiv:2010.08423](https://arxiv.org/abs/2010.08423).

- [50] A.-S. Himmel, M. Bentert, A. Nichterlein, and R. Niedermeier, Efficient computation of optimal temporal walks under waiting-time constraints, in *International Conference on Complex Networks and Their Applications* (Springer, New York, 2019), pp. 494–506.
- [51] D. R. De Souza and T. Tomé, Stochastic lattice gas model describing the dynamics of the SIRS epidemic process, *Physica A (Amsterdam)* **389**, 1142 (2010).
- [52] M. Kivelä, J. Cambe, J. Saramäki, and M. Karsai, Mapping temporal-network percolation to weighted, static event graphs, *Sci. Rep.* **8**, 12357 (2018).
- [53] A. Badie-Modiri, A. K. Rizi, M. Karsai, and M. Kivelä, Directed percolation in random temporal network models with heterogeneities, *Phys. Rev. E* **105**, 054313 (2022).
- [54] H. H. K. Lentz, T. Selhorst, and I. M. Sokolov, Unfolding Accessibility Provides a Macroscopic Approach to Temporal Networks, *Phys. Rev. Lett.* **110**, 118701 (2013).
- [55] A. Mellor, Event graphs: Advances and applications of second-order time-unfolded temporal network models, *Adv. Complex Syst.* **22**, 1950006 (2019).
- [56] J. Saramäki, M. Kivelä, and M. Karsai, Weighted temporal event graphs, in *Temporal Network Theory* (Springer, New York, 2019), pp. 107–128.
- [57] L. Kovanen, M. Karsai, K. Kaski, J. Kertész, and J. Saramäki, Temporal motifs in time-dependent networks, *J. Stat. Mech.* (2011) P11005.
- [58] A. Mellor, Analysing collective behaviour in temporal networks using event graphs and temporal motifs, [arXiv:1801.10527](https://arxiv.org/abs/1801.10527).
- [59] M. Torricelli, M. Karsai, and L. Gauvin, weg2vec: Event embedding for temporal networks, *Sci. Rep.* **10**, 7164 (2020).
- [60] A. Mellor, The temporal event graph, *J. Complex Networks* **6**, 639 (2018).
- [61] See Supplemental Material at <http://link.aps.org/supplemental/10.1103/PhysRevResearch.4.L022047> for details on proofs and description of datasets.
- [62] P. Grassberger, On phase transitions in Schlögl's second model, *Z. Phys. B* **47**, 365 (1982).
- [63] H. K. Janssen, On the nonequilibrium phase transition in reaction-diffusion systems with an absorbing stationary state, *Z. Phys. B* **42**, 151 (1981).
- [64] M. E. J. Newman, S. H. Strogatz, and D. J. Watts, Random graphs with arbitrary degree distributions and their applications, *Phys. Rev. E* **64**, 026118 (2001).
- [65] P. Grassberger and A. De La Torre, Reggeon field theory (Schlögl's first model) on a lattice: Monte Carlo calculations of critical behaviour, *Ann. Phys. (Amsterdam)* **122**, 373 (1979).
- [66] Bureau of Transportation Statistics, Bureau of Transportation Statistics website (2017), <https://www.bts.gov/>.
- [67] R. Kujala, C. Weckström, R. K. Darst, M. N. Mladenović, and J. Saramäki, A collection of public transport network data sets for 25 cities, *Sci. Data* **5**, 180089 (2018).
- [68] J. Yang and J. Leskovec, Patterns of temporal variation in online media, in *Proceedings of the Fourth ACM International Conference on Web Search and Data Mining* (ACM, New York, 2011), pp. 177–186.
- [69] M. Karsai, M. Kivelä, R. K. Pan, K. Kaski, J. Kertész, A.-L. Barabási, and J. Saramäki, Small but slow world: How network topology and burstiness slow down spreading, *Phys. Rev. E* **83**, 025102(R) (2011).
- [70] S. N. Dorogovtsev, A. V. Goltsev, and J. F. F. Mendes, Critical phenomena in complex networks, *Rev. Mod. Phys.* **80**, 1275 (2008).
- [71] D. R. Chialvo, Emergent complex neural dynamics, *Nat. Phys.* **6**, 744 (2010).
- [72] J. Hesse and T. Gross, Self-organized criticality as a fundamental property of neural systems, *Front. Syst. Neurosci.* **8**, 166 (2014).
- [73] C.-W. Shin and S. Kim, Self-organized criticality and scale-free properties in emergent functional neural networks, *Phys. Rev. E* **74**, 045101(R) (2006).
- [74] P. Bak and C. Tang, Earthquakes as a self-organized critical phenomenon, *J. Geophys. Res.: Solid Earth* **94**, 15635 (1989).
- [75] Y. Chen and Y. Zhou, Scaling laws and indications of self-organized criticality in urban systems, *Chaos, Solitons Fractals* **35**, 85 (2008).
- [76] P. Bak, C. Tang, and K. Wiesenfeld, Self-Organized Criticality: An Explanation of the $1/f$ Noise, *Phys. Rev. Lett.* **59**, 381 (1987).
- [77] P. Bak, C. Tang, and K. Wiesenfeld, Self-organized criticality, *Phys. Rev. A* **38**, 364 (1988).
- [78] B. Blasius, Power-law distribution in the number of confirmed COVID-19 cases, *Chaos* **30**, 093123 (2020).
- [79] J. Leitch, K. A. Alexander, and S. Sengupta, Toward epidemic thresholds on temporal networks: a review and open questions, *Appl. Network Sci.* **4**, 105 (2019).
- [80] A. Barrat, C. Cattuto, M. Kivelä, S. Lehmann, and J. Saramäki, Effect of manual and digital contact tracing on COVID-19 outbreaks: a study on empirical contact data, *J. R. Soc. Interface* **18**, 20201000 (2021).